Silencing profilin-1 inhibits endothelial cell proliferation, migration and cord morphogenesis

Zhijie Ding, Anja Lambrechts, Mayur Parepally and Partha Roy

Journal of Cell Science 119, 4366 (2006) doi:10.1242/jcs.03268

There was an error published in *J. Cell Sci.* **119**, 4127-4137.

In the e-press version of this paper that was published on 12 September 2006, the labels in Fig. 5B were incorrect. Both the published print and online versions of this article are correct.

The correct figure is shown below.

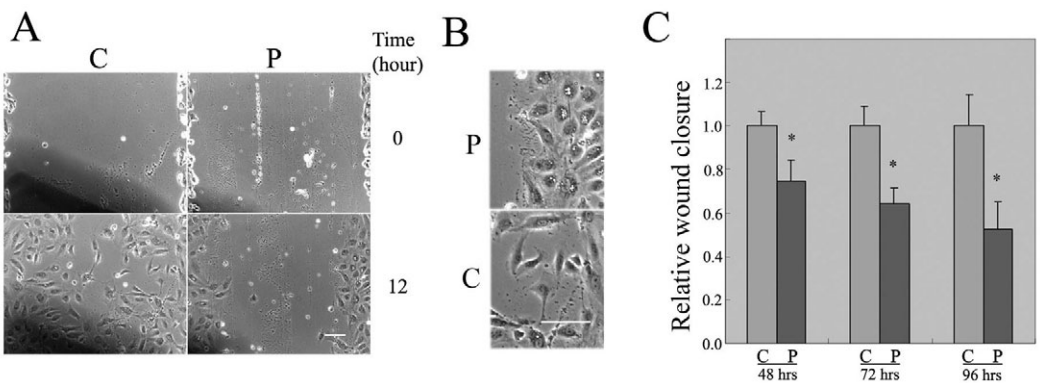

The authors apologise for this mistake.

Silencing profilin-1 inhibits endothelial cell proliferation, migration and cord morphogenesis

Zhijie Ding[1], Anja Lambrechts[2], Mayur Parepally[3] and Partha Roy[1,4,*]

[1]Department of Bioengineering, University of Pittsburgh, 749 Benedum Hall, 3700 O'Hara Street, Pittsburgh, PA 15261, USA
[2]Department of Biochemistry, Ghent University, Albert Baertsoenkaai 3, 9000 Ghent, Belgium
[3]Department of Biological Sciences, Carnegie Mellon University, 4400 Fifth Avenue, Pittsburgh, PA 15213, USA
[4]Department of Pathology, University of Pittsburgh, School of Medicine, S-417 BST, 200 Lothrup Street, Pittsburgh, PA 15261, USA
*Author for correspondence (e-mail: proy@engr.pitt.edu)

Accepted 20 July 2006
Journal of Cell Science 119, 4127-4137 Published by The Company of Biologists 2006
doi:10.1242/jcs.03178

Summary

Expression of several actin-binding proteins including profilin-1 is up-regulated during capillary morphogenesis of endothelial cells, the biological significance of which remains unknown. Specifically, we hypothesized that profilin-1 is important for endothelial migration and proliferation. In this study, we suppressed profilin-1 expression in human umbilical vein endothelial cells by RNA-interference. Gene silencing of profilin-1 led to significant reduction in the formation of actin filaments and focal adhesions. Loss of profilin-1 expression was also associated with reduced dynamics of cell-cell adhesion. Data from both wound-healing experiments and time-lapse imaging of individual cells showed inhibition of cell migration when profilin-1 expression was suppressed. Cells lacking profilin-1 exhibited defects in membrane protrusion, both in terms of its magnitude and directional persistence. Furthermore, loss of profilin-1 expression inhibited cell growth without compromising cell survival, at least in the short-term, thus suggesting that profilin-1 also plays an important role in endothelial proliferation as hypothesized. Finally, silencing profilin-1 expression suppressed matrigel-induced early cord morphogenesis of endothelial cells. Taken together, our data suggest that profilin-1 may play important role in biological events that involve endothelial proliferation, migration and morphogenesis.

Key words: Profilin-1, Endothelial cells, Morphogenesis, Migration, Proliferation, Adhesion

Introduction

Angiogenesis, a process of capillary outgrowth from preexisting vessels, plays a pivotal role in various physiological adaptations and pathological conditions including wound healing, coronary heart disease, diabetic retinopathy and growth of solid tumors (Carmeliet and Jain, 2000; Yancopoulos et al., 2000). During angiogenesis, endothelial cells (ECs) organize to form three-dimensional (3D) capillary networks, which encompasses a range of cellular processes including activation, protease production, migration, proliferation and differentiation of ECs (Kanda et al., 2004; Whelan and Senger, 2003). The exact molecular details how ECs physically assemble into capillary structures are not completely understood. Over the years, studies using in vitro models where ECs plated either on reconstituted basement membrane or embedded in 3D collagen matrices form polygonal network of pre-capillary cords (akin to the capillary structures in vivo) have been utilized to investigate different aspects of EC morphogenesis (Davis et al., 2002). Those studies indicate that extracellular matrix (ECM)-integrin interactions and signaling events involving cytoskeletal elements that control EC migration and shape change, now collectively termed as MIC (matrix-integrin-cytoskeleton) signaling axis, drive the capillary morphogenesis of ECs (Davis et al., 2002; Davis et al., 2000; Davis and Camarillo, 1995).

Marked changes in cell shape and migration that accompany capillary morphogenesis of ECs imply active reorganization of the actin cytoskeleton (Davis et al., 2002). Remodeling of actin cytoskeleton is controlled by several different classes of actin-binding proteins (ABPs) including those involved in monomer sequestering, nucleating, filament-severing, depolymerizing, and capping activities (Pollard and Borisy, 2003). However, only a handful of studies have been reported to date that directly examined the role of various ABPs in morphogenetic events of ECs. Subtractive cDNA cloning of ECs plated on matrigel first detected increased expression of thymosin β4 [a G (globular)-actin sequestering protein] (Grant et al., 1995), which was later shown to be a potent stimulator of angiogenesis (Cha et al., 2003; Grant et al., 1999; Malinda et al., 1997; Philp et al., 2004). Similarly, a previous study reported up-regulation in the expression of profilin-1 (Pfn1, a ubiquitously expressed ABP encoded by the Pfn family of genes) during capillary morphogenesis (Salazar et al., 1999), the biological significance of which, however, remains unknown.

Four distinct Pfn genes have been identified so far: *Pfn1*, *Pfn2* [two splice variants of Pfn2 exist that are mainly found in nerve cells (Di Nardo et al., 2000; Kwiatkowski and Bruns, 1988; Lambrechts et al., 2000)]; *Pfn3* [kidney and testis specific (Hu et al., 2001)]; and *Pfn4* [testis specific (Obermann et al., 2005)]. Although Pfn1 was originally identified as a G-actin sequestering protein (Carlsson et al., 1977), depending upon the conditions, it can either sequester G-actin and hence inhibit actin polymerization, or promote actin assembly

(Schluter et al., 1997). Since the intracellular concentration of Pfn1 does not appear to be sufficient to account for the high G-actin content in most cells, its role as a promoter of actin polymerization is currently favored. Pfn1 promotes actin assembly via its ability to accelerate nucleotide exchange (ADP to ATP) on G-actin and shuttle Pfn-actin (ATP-bound) complex to free barbed ends of actin filaments (Witke, 2004). Besides actin, Pfn1 binds to phosphoinositides [mainly phosphatidylinositol-4,5-bisphosphate (PIP_2) and phosphatidylinositol-3,4,5-triphosphate (PIP_3)] and a plethora of proline-rich ligands ranging from those that directly stimulate actin assembly in response to extracellular signals [example: proteins belonging to Vasodilator Stimulated Phosphoprotein or VASP (Reinhard et al., 1995), Wiskott-Aldrich Syndrome Protein or WASP (Suetsugu et al., 1998) and Diaphanous (Watanabe et al., 1997) families] to ones involved in endocytosis, gene splicing and transcription (Witke, 2004).

Gene deletion of both *Pfn1* and *Pfn2* causing impaired motility and cytokinesis of *Dictyostelium* amebae produced the first direct evidence of Pfn's involvement in migration and proliferation of lower eukaryotic cells (Haugwitz et al., 1994). Defects in cell proliferation and migration were also evident in *chickadee* (a Pfn1-homolog)-null mutants of *Drosophila* where a late-stage embryonic lethality was observed (Verheyen and Cooley, 1994). Due to a very early-stage embryonic lethality resulting from Pfn1-gene knockout in mice (Witke et al., 2001), similar studies have not been performed to date to explore whether lack of Pfn1 has any overall impact on the migration of mammalian cells. Lack of viability of Pfn1-null embryos nevertheless suggests Pfn1's role in proliferation and/or survival for mammalian cells. Pfn1's function has been extensively studied in pathogen-based model systems where it plays an important role in promoting the intracellular movement of bacterial pathogens (Grenklo et al., 2003; Laurent et al., 1999; Mimuro et al., 2000; Sanger et al., 1995; Theriot et al., 1994). Since host-cell induced movement of pathogens is a molecular mimicry of actin polymerization at the leading edge of migrating cells, it is thought that one of Pfn1's function is to facilitate actin assembly during cell protrusion. This notion is further supported by several other studies demonstrating Pfn1's involvement in the formation of actin-based protrusive structures (Hajkova et al., 2000; Suetsugu et al., 1998; Suetsugu et al., 1999) as well as its preferential localization at the protrusive edge (Buss et al., 1992; Chou et al., 2002; Neely and Macaluso, 1997; Neuhoff et al., 2005). Given Pfn1's importance in cell migration and proliferation, it is thus intriguing that Pfn1 expression is conspicuously down-regulated in aggressive mammary and pancreatic carcinoma cells when compared with their normal counterparts (Gronborg et al., 2006; Janke et al., 2000). Suppression of growth (Janke et al., 2000) and migration (Roy and Jacobson, 2004) of mammary carcinoma cells induced by overexpression of Pfn1 further suggest that Pfn1's role in mammalian cell migration and proliferation may be complex and cell-type dependent.

Based on significant up-regulation of Pfn1 expression in human umbilical vein endothelial cells (HUVECs) during capillary morphogenesis (Salazar et al., 1999), one envisions that Pfn1 might play an instrumental role during endothelial morphogenesis. Related to this, we specifically hypothesized that Pfn1's function is important for EC migration and proliferation. In the present study, we tested this hypothesis by examining the effects of suppression of Pfn1 expression on EC proliferation and migration. We further assessed whether loss of Pfn1 expression affects ECM-induced early morphogenesis of ECs.

Results

Silencing Pfn1 alters the actin cytoskeleton, cell-matrix and cell-cell adhesions in HUVECs

To suppress Pfn1 expression, we adopted transient transfection of HUVECs with either a non-targeting control (C) or Pfn1-specific (P) siRNA construct. Initially, to determine the specificity of Pfn1-siRNA, we transiently transfected the siRNA constructs into MDA-MB-231 breast carcinoma cells, which were genetically engineered by us to provide stable expression of different point-mutants of GFP-Pfn1. These mutants involved a 2 base-pair alteration either within (mutant-1) or outside (mutant-2) the region targeted by Pfn1-siRNA. As judged by the decrease in GFP-fluorescence, our Pfn1-siRNA down-regulated the expression of mutant-2 as expected, but was ineffective in suppressing the expression of mutant-1. In negative control experiments, Pfn1-siRNA treatment did not non-specifically decrease the fluorescence of GFP-expressing MDA-MB-231 cells (Fig. 1A). Taken together, these data thus demonstrate the specificity of action of our Pfn1-siRNA. The bar graph in Fig. 1B displays the silencing efficiency of Pfn1-siRNA in HUVECs as a function of time (48-96 hours), which shows a time-dependent progressive loss of Pfn1 expression with ~97% gene-silencing achieved 96 hours after transfection. The representative Pfn1 immunoblots at different time-points after transfection are shown in the inset of Fig. 1B (the GAPDH blot serves as the loading control). We have also confirmed that the polyclonal Pfn1 antibody used in this study is specific and does not cross-react with Pfn2 (data not shown). We could not detect Pfn2 expression by immunoblotting under either of the experimental conditions (inset of Fig. 1B) thus suggesting that there is no compensatory up-regulation of Pfn2 when Pfn1 expression is suppressed in HUVECs.

The effect of silencing Pfn1 on endothelial actin cytoskeleton was next evaluated by rhodamine-phalloidin staining of HUVECs 96 hours after transfection, which showed that cells bearing Pfn1-siRNA have significantly less actin filaments, particularly those comprising stress-fibers, compared with the control-siRNA transfected cells (Fig. 1C). Quantification of phalloidin-fluorescence showed approximately 29% reduction in the overall F-actin content of HUVECs due to loss of Pfn1 expression (Fig. 1D). Since Pfn1 has been recently implicated in gene transcription (Lederer et al., 2005), we next asked whether expression levels of actin and some of the ABPs that are important for actin assembly in response to growth factor signaling such as VASP, N-WASP and mDia1 are altered as a result of silencing Pfn1. Immunoblots of whole cell lysates showed no appreciable change in the expression levels of actin and the indicated ABPs at any time-point after transfection (Fig. 1E). Taken together, these data suggest that loss of Pfn1 expression alters actin cytoskeleton via direct modulation of actin polymerization and/or bundling of actin filaments.

Since both cell-matrix and cell-cell adhesion complexes physically associate with actin cytoskeleton, we next asked

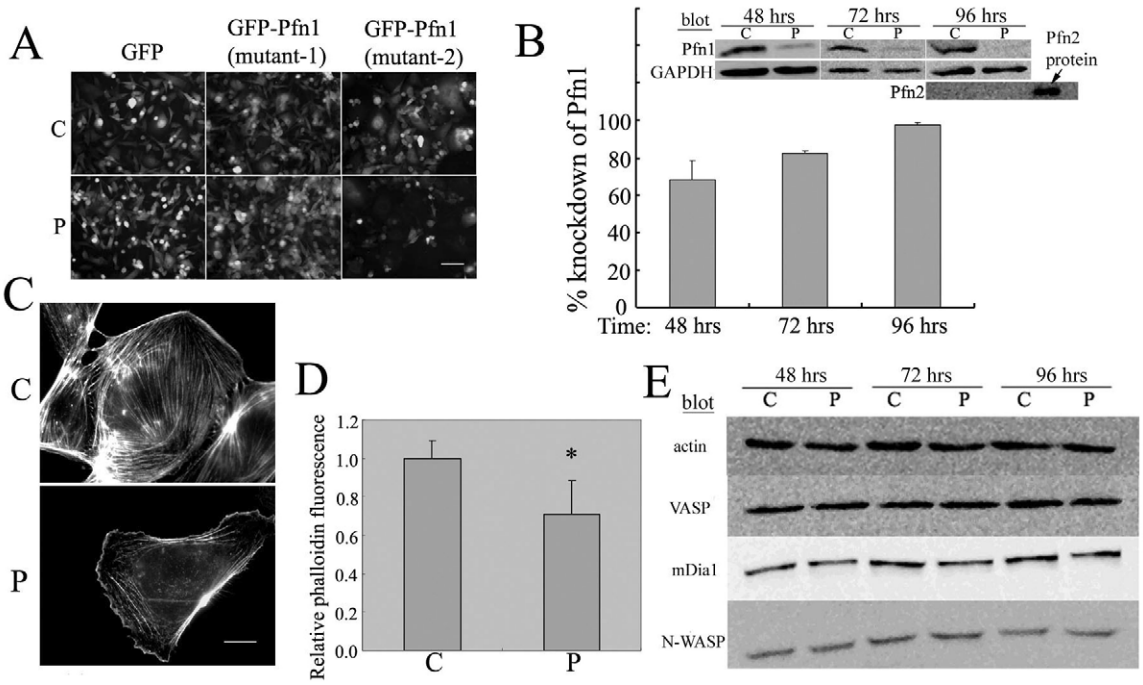

Fig. 1. Silencing Pfn1 expression affects the actin cytoskeleton in HUVECs: (A) Target specificity of Pfn1-siRNA was initially demonstrated by transfecting either control (C) or Pfn1-specific (P) siRNAs in MDA-MB-231 breast cancer cells that stably express either GFP or different point-mutants of GFP-Pfn1 (designated as mutant-1 and mutant-2 that carried a 2-base-pair alteration both within and outside of the targeting region of Pfn1-siRNA, respectively). Fluorescence micrographs of cells show that Pfn1-siRNA suppresses the expression of mutant-2, but not of mutant-1. Fluorescence of control GFP-expressing cells is not affected by Pfn1-siRNA treatment. Bar, 150 μm. (B) A bar graph shows time-dependent progressive loss of Pfn1 expression with nearly 97% suppression of Pfn1 expression 96 hours after Pfn1-siRNA transfection (data summarized based on immunoblot analyses of HUVEC extracts from three independent experiments). The inset shows the actual representative Pfn1-immunoblots of HUVEC extracts prepared at different time-points after siRNA transfection with GAPDH blot serving as the loading control. Additional immunoblot data shows no detectable Pfn2 expression under either experimental condition (purified Pfn2 serves the positive control for the immunoblot). (C) Rhodamine-phalloidin staining of HUVECs shows that silencing Pfn1 dramatically inhibits the formation of actin stress-fibers. Bar, 20 μm. (D) A bar graph displaying the relative (normalized with respect to the control cells) fluorescence intensity of phalloidin shows a 29% decrease in the average level of F-actin in Pfn1-deficient cells. These data were obtained from analyses of 640 control and 584 Pfn1-deficient cells from two independent experiments, the difference of which was found to be statistically significant (the asterisk indicates $P<0.0001$). (E) Immunoblots show comparable expression levels of actin and several ABPs such as VASP, mDia1, and N-WASP at 48, 72 and 96 hours after transfection.

whether loss of Pfn1 expression has any impact on either kind of adhesive structures in ECs. Previous data showed that Pfn1-overexpression causes human aortic ECs to form more focal contacts and display increased adhesion on fibronectin-substrate (Moldovan et al., 1997) thus suggesting a possible role of Pfn1 in regulating cell-matrix adhesion. To further this line of inquiry, we performed vinculin [a marker for focal adhesion (FA)] immunostaining of HUVECs, which showed a marked inhibition of FA assembly when Pfn1 expression was silenced (Fig. 2A). A bar graph in Fig. 2B summarizes the results from quantitative analyses of vinculin-staining data, which showed significantly lower FA density (defined as the number of FA plaques per 100 μm^2 of cell area) in Pfn1-deficient cells (2.7±1.9) when compared with control cells (6.1±2.1). The FAs observed for the control cells also appeared to be larger in size compared with those in Pfn1-deficient cells. Overall, these data demonstrate that Pfn1 plays an important role in regulating cell-matrix adhesions in ECs.

Whether Pfn1 is involved in regulating cell-cell adhesion has not been explored at all. Interestingly, yeast-two hybrid screening technique has previously identified Pfn1 as a binding partner for AF-6, a multidomain protein that is localized at cell-cell junctions (Boettner et al., 2000). However, the functional significance of such interaction remains unknown. To determine whether loss of Pfn1 expression affects endothelial cell-cell junctions, confluent monolayers of serum-starved HUVECs, carrying either control or Pfn1-siRNA, were subjected to VEGF (a potent disruptor of endothelial cell-cell junctions) stimulation and immunostaining of VE-cadherin (a marker for adherence junction) and ZO-1 (a marker for tight junction) were performed. As expected, VEGF stimulation caused significant loss of junctional staining of both VE-cadherin and ZO-1 (arrows) with concomitant creation of paracellular holes (arrowheads) in the monolayer of control cells (Fig. 2C,D). Interestingly, VEGF-induced delocalization of both VE-cadherin and ZO-1 from the cell-cell junctions was significantly inhibited in Pfn1-deficient cells (Fig. 2C,D). Although the baseline (i.e. under serum-starved state) staining pattern of VE-cadherin was similar for both control and Pfn1-deficient cells, subtle differences in ZO-1 staining were apparent between the two experimental conditions. For example, control cells had somewhat more fragmented junctional and higher nuclear

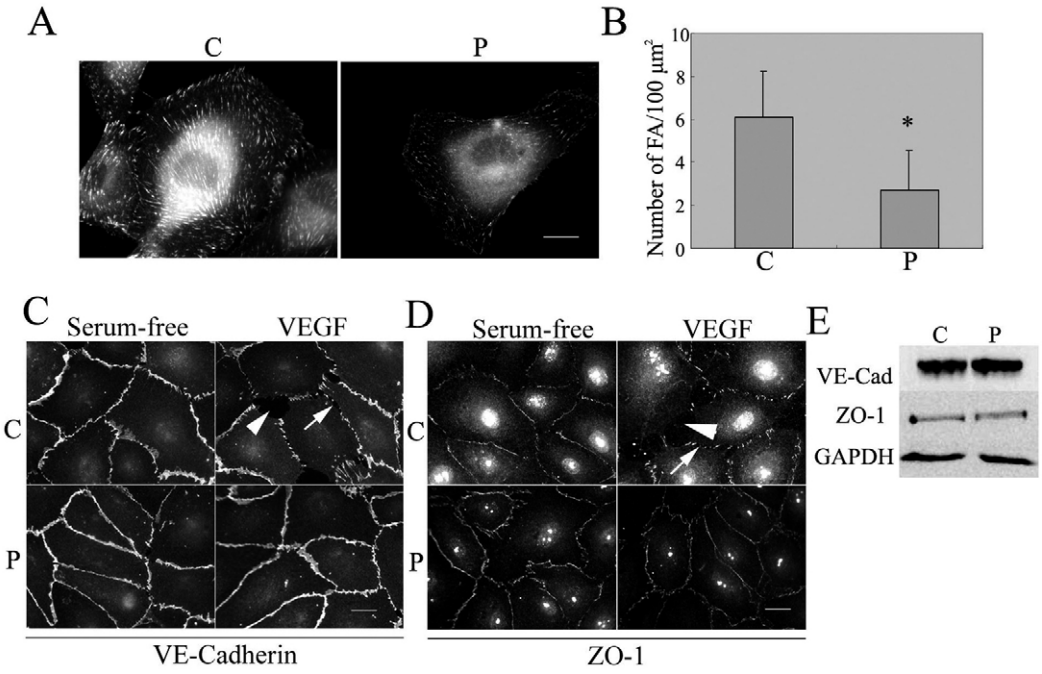

Fig. 2. Loss of Pfn1 expression alters cell-matrix and cell-cell adhesions in HUVECs: (A) Vinculin-immunostaining shows a dramatic reduction in FA formation when Pfn1 expression is silenced (C, control siRNA; P, Pfn1-siRNA). Bar, 20 μm. (B) A bar graph shows a significantly (P<0.001) higher FA density (number of FA/100 μm^2 of cell area) in control cells (6.1±2.1) than in Pfn1-deficient cells (2.7±1.9). These data are based on analyses of 56 control and 69 Pfn1-deficient cells that were randomly selected from two independent experiments. (C,D) VE-cadherin and ZO-1 immunostaining show that VEGF stimulation causes loss of junctional staining of these proteins (arrow) and creation of paracellular holes (arrowhead) in control cells. VEGF-induced delocalization of VE-cadherin and ZO-1 from cell-cell junctions is significantly inhibited in Pfn1-deficient ECs. Bar, 20 μm. (E) Immunoblot data show no appreciable change in the expression of VE-cadherin and ZO-1 between control and Pfn1-siRNA treated cells (the GAPDH blot serves as the loading controls).

staining of ZO-1. Immunoblot data showed no appreciable change in the expression level of either VE-cadherin or ZO-1 between the two experimental conditions (Fig. 2E). These results suggest that loss of Pfn1 expression suppresses VEGF-induced dynamics of cell-cell adhesions in ECs.

Pfn1 regulates HUVEC proliferation

To test our hypothesis that Pfn1 plays a role in EC proliferation, we next compared cell growth at different time-points (48-96 hours) after siRNA transfection, which showed that Pfn1-siRNA treatment led to nearly 42% inhibition in HUVEC growth when compared with the control transfection condition (Fig. 3A). Inhibition in cell growth was evident within 48 hours after transfection. From nuclear staining of cells with DAPI, we did not detect any ECs with multinuclei (>2) phenotype thus suggesting no gross defect in cytokinesis as a result of lack of Pfn1 expression. We also wanted to see whether a difference in the number of apoptotic cells (display nuclear fragmentation in DAPI staining) between the two culture conditions might explain the differential cell-growth. The nuclear morphology of both control and Pfn1-deficient cells appeared completely normal (Fig. 3B), and the number of apoptotic cells in the culture was absolutely negligible (<0.5%) in either case. These data suggest that loss of Pfn1 expression does not compromise HUVEC survival, at least in the short term, and hence, reduced cell growth in Pfn1-siRNA treated culture was most likely due to diminished proliferative capacity of these cells.

Loss of Pfn1 inhibits HUVEC spreading

Since Pfn1 has been shown to play an important role in forming actin-based protrusive structures, we next evaluated whether early cell spreading (an event that involves active cell protrusion), on ECM-coated substrate is affected by loss of

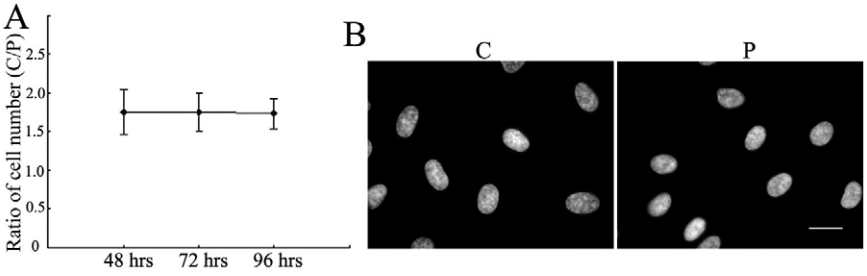

Fig. 3. Silencing Pfn1 expression inhibits cell growth: (A) A line graph shows the ratio of the number of control (denoted by 'C') to that of Pfn1-deficient cells (denoted by 'P') in culture at 48, 72 and 96 hours after transfection. (These data were summarized from three independent experiments and P<0.0002.) (B) DAPI staining of cells shows normal nuclear morphology under either experimental condition. Bar, 20 μm.

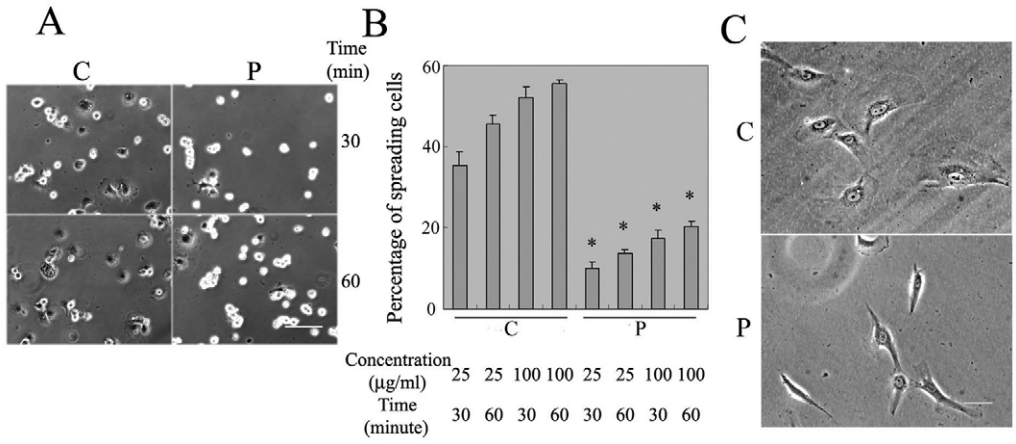

Fig. 4. Loss of Pfn1 expression affects HUVEC spreading: (A) Phase contrast images of HUVECs seeded 1 hour after plating on a substrate that is pre-coated with 100 μg/ml matrigel show higher proportion of spreading cells (appear phase dense) in the control group (denoted by 'C'). Impaired cell spreading was evident from round morphology of majority of Pfn1-deficient cells (denoted by 'P'). Bar, 100 μm. (B) A bar graph plotting the percentage of spreading cells at two different time-points (30 minutes and 1 hour) and for two different coating concentrations of matrigel clearly shows increased spreading efficiency of the control cells (these data were pooled from the analyses of approximately 800-1000 cells for each experimental condition from two independent experiments). The asterisk indicates $P<0.001$. (C) Pfn1-deficient cells were still found to be much less flat and spread-out compared with the control cells at 22 hours after cell-seeding on matrigel-coated substrates. Bar, 50 μm.

Pfn1 expression. Fig. 4A shows the morphology of HUVECs on matrigel (100 μg/ml)-coated substrate within 1 hour after plating. From phase contrast images where spreading cells appear darker (phase-dense), it is evident that Pfn1-deficient cells are much less efficient in spreading when compared with the control cells. Fig. 4B summarizes the data in the form of a bar graph plotting the percentage of spreading cells on substrates coated with different concentrations of matrigel. Although a higher concentration of matrigel generally facilitated cell spreading, a 3-fold decrease in the spreading efficiency was observed when Pfn1 expression was silenced, thus further confirming that Pfn1 plays a key role in regulating EC protrusion. To further determine whether loss of Pfn1 actually inhibits or only delays cell spreading, we compared HUVEC-morphology on matrigel–coated substrates at later time-points. Even at 22 hours after cell-seeding, the extent of spreading of Pn1-deficient cells was clearly much less compared with that of control cells (Fig. 4C), therefore meaning that silencing Pfn1 actually inhibits cell spreading.

Pfn1 is important for HUVEC migration

To test our hypothesis that Pfn1's function is important for EC migration, we next examined whether directed migration of HUVECs is affected by loss of Pfn1 expression using a standard wound-healing assay. Fig. 5A depicts the results of a typical wound-healing experiment performed 96 hours after siRNA transfection, where Pfn1-deficient cells clearly showed significant impairment in wound closure when compared with the control cells. At the wound margins, control ECs were seen as isolated cells, whereas Pfn1-deficient cells appeared to

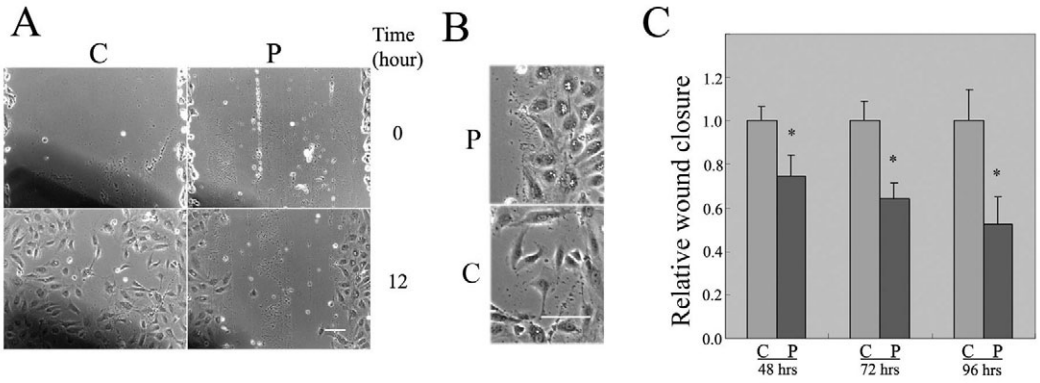

Fig. 5. Loss of Pfn1 inhibits HUVEC migration in wound healing assay. (A) Representative images of the wound margins immediately and 12 hours after wounding show significant impairment in wound closure by HUVECs due to loss of Pfn1 expression (C, control siRNA; P, Pfn1-siRNA). Bar, 100 μm. (B) A higher magnification of the wound margin indicates closer association of Pfn1-deficient cells. Bar, 100 μm. (C) A bar graph plotting the relative efficiency of wound closure shows Pfn1-siRNA treatment inhibited wound-closure by 25%, 36% and 47% when evaluated at 48, 72 and 96 hours after transfection, respectively. (These data are summarized from three independent experiments and the asterisk indicates $P<0.002$.)

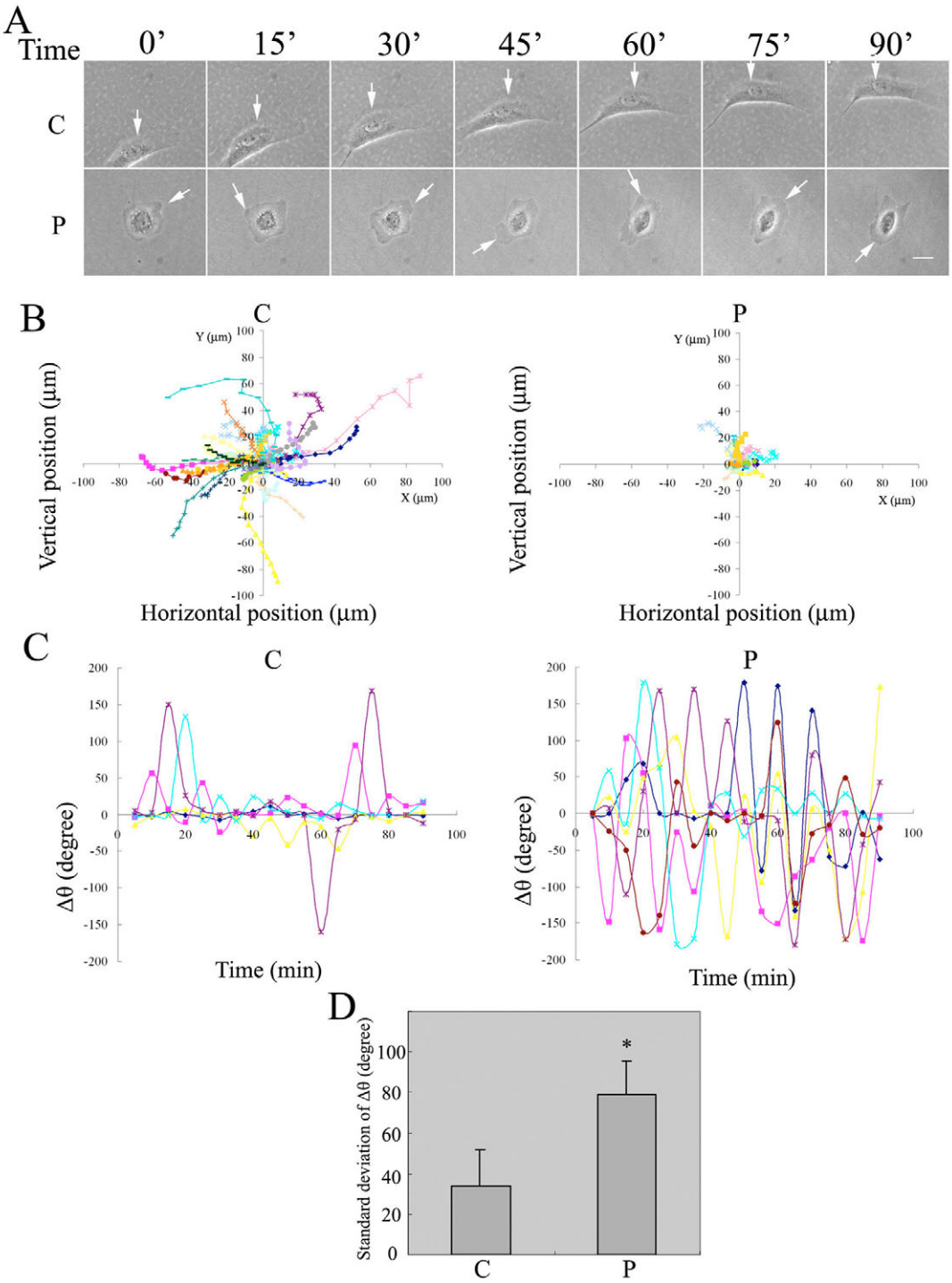

Fig. 6. Effect of silencing Pfn1 expression on single cell migration: (A) A typical time-lapse imaging experiment shows directed migration of control cells (denoted by 'C') involving directed protrusion and significant net cell translocation. By contrast, Pfn1-deficient cells (denoted by 'P') produce small, randomly directed protrusion with much less net cell translocation (the direction of protrusion is indicated by the arrow). Bar, 30 μm. (B) Trajectories of individual cells from the frame-by-frame analyses of the centroid of cell nuclei show a significantly (P<0.001) larger net distance traveled by the control cells (43.6±26.0 μm) compared with the Pfn1-deficient cells (11.3±9.6 μm) during the 90-minute observation period (migration data of 27 control and 21 Pfn1-deficient cells from a total of three independent experiments were pooled for the analysis). (C) Representative plots of change in protrusion direction between successive image frames (Δθ) from a typical experiment are shown side-by-side to display much larger oscillation of Δθ in Pfn1-deficient cells (these plots were generated based on motility data of five control and six Pfn1-deficient cells in one experiment). (D) The bar graph compares the standard deviation values of Δθ for the entire 90-minute observation period (these data are based on the average values calculated for 14 control and 19 Pfn1-deficient cells – those cells that either barely protruded or came in contact with a neighboring cell at any point during the course of the experiment were excluded from the analysis). The asterisk indicates P<0.0001.

maintain connections with the neighboring cells (Fig. 5B). This distinctive feature also seems to be consistent with reduced dynamics of cell-cell adhesions in Pfn1-deficient cells as previously demonstrated in Fig. 2C,D. A bar graph in Fig. 5C summarizes the wound-healing data as a function of time where Pfn1-siRNA treatment inhibited wound-closure by 25%, 36%, and 47% at 48, 72 and 96 hours after transfection, respectively. These data thus demonstrate increasing inhibition of HUVEC migration with progressive loss of Pfn1 expression.

Cell migration in a monolayer set-up, as in a wound-healing assay, can be affected by the strength of cell-cell adhesion. Since our data suggested Pfn1-dependent alteration in cell-cell adhesion, we additionally performed time-lapse imaging of individual HUVECs to determine whether intrinsic EC migration is affected by loss of Pfn1 expression. Fig. 6A shows the results of a typical set of time-lapse experiments where HUVECs bearing control-siRNA displayed directed migration involving significant translocation of their cell bodies during the course of the experiment (upper panel). Consistent with our findings from wound-healing experiments, a marked inhibition in random cell migration was observed in the case of Pfn1-deficient cells (lower panel). The single-cell migration data are summarized in Fig. 6B, which depicts the trajectories of individual cells obtained by frame-by-frame analyses of the centroid positions of cell-nuclei (assumed to be the representations of cell-bodies in this case). The average net distances translocated by the control and Pfn1-deficient cells in the 90-minute observation period were 43.6±26.0 μm (n=27 cells) and 11.3±9.6 μm (n=21 cells), respectively, the difference of which was found to be statistically significant (P<0.001). Overall, the results from wound-healing and time-lapse imaging experiments clearly demonstrate that Pfn1 plays an important role in EC migration as hypothesized.

Our time-lapse imaging data also showed a difference in the protrusive activity between the control and Pfn1-siRNA treated cells. While control cells mostly maintained persistence in the direction of protrusion, cells bearing Pfn1-siRNA typically exhibited smaller and random protrusions that lacked any directional bias (the direction of protrusion at any instance is marked by an arrow; see Fig. 6A). To represent the differences in the protrusive behavior between the two experimental conditions in a quantitative fashion, we then analyzed and plotted the change in the direction of protrusion between successive image frames ($\Delta\theta_i=\theta_i-\theta_{i-1}$, where θ_i denotes the direction of protrusion at the i-th image frame) as a function of time during the entire 90-minute course of experiment for each cell. Representative plots based on data analyses of control and Pfn1-deficient cells from a typical experiment are shown side-by-side in Fig. 6C, where clearly a much larger oscillation of $\Delta\theta$, thus meaning a decreased directional persistence of protrusion, was seen when Pfn1 expression was suppressed. To summarize the persistence data, the standard deviation of $\Delta\theta$ for the 90-minute time-lapse period (a higher value of such index would correlate with decreased directional persistence of protrusion) was calculated for individual cells, pooled and then averaged based on the total number of cells analyzed from three independent experiments. A nearly 2.3-fold higher value of this index determined for Pfn1-deficient cells (Fig. 6D) further confirms a decreased ability of these cells to sustain directed protrusion when compared with the control cells.

It has been previously shown that membrane targeting of VASP to the leading edge decreases the persistence of protrusion in migrating cells (Bear et al., 2002). To further study whether VASP localization in migrating HUVECs is altered when Pfn1 expression is suppressed, we performed VASP-immunostaining of HUVECs in a wound-healing set-up, the results of which are shown in Fig. 7. We were specifically interested in VASP localization for cells situated at the wound-edge, since those cells are capable of executing directed migration with least obstructed membrane protrusion. In control HUVECs, VASP predominantly localized at the FAs and actin stress-fibers. At the leading edge, a much stronger VASP staining was observed in Pfn1-deficient cells when compared with the control cells, thus suggesting that loss of Pfn1 expression in HUVECs is associated with increased membrane targeting of VASP.

Silencing Pfn1 inhibits ECM-induced cord formation by HUVECs

To finally determine whether Pfn1 plays any role in the early

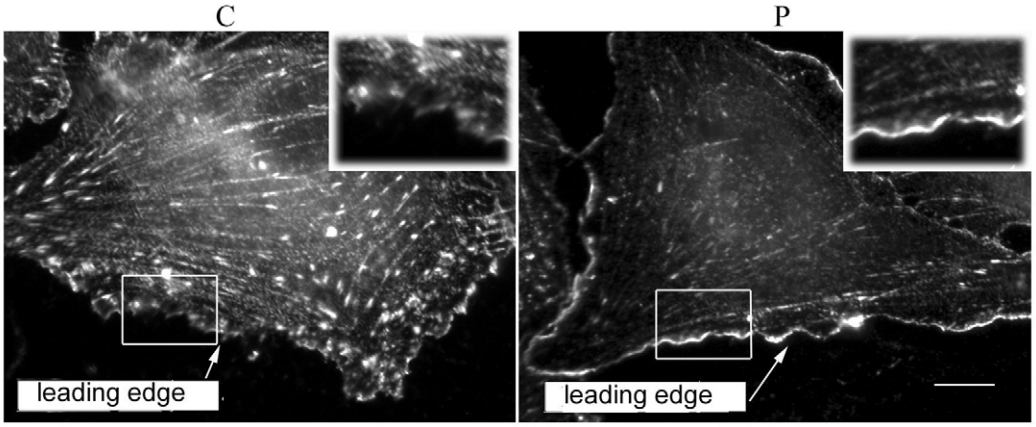

Fig. 7. Silencing Pfn1 alters the localization of VASP in migrating HUVECs. In control cells (denoted by 'C'), VASP is predominantly localized at the focal adhesions and actin stress-fibers, and has a punctate distribution at the leading edge. Pfn1-deficient cells (denoted by 'P') have much stronger localization of VASP at the leading edge. The inset in each panel shows a magnified view of the boxed region depicting differences in VASP localization at the leading edge between the two experimental conditions. Bar, 10 μm.

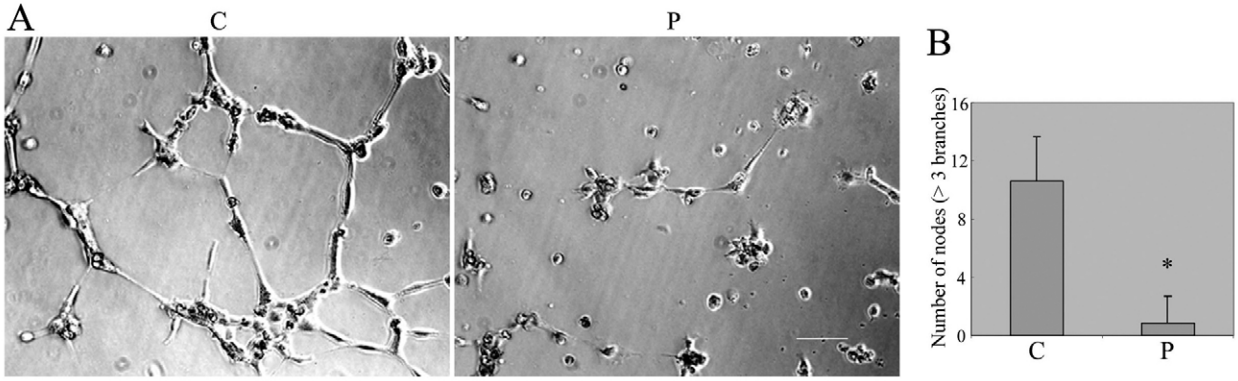

Fig. 8. Effect of silencing Pfn1 on early cord morphogenesis of HUVECs. (A) Control HUVECs (denoted by 'C') form prominent cord-like structures on polymerized matrigel by 8 hours after plating. Cord formation is significantly inhibited in the case of Pfn1-deficient cells (denoted by 'P'). Bar, 100 μm. (B) A bar graph shows significantly higher number of nodes involving at least three branches in the control cells compared with the same in Pfn1-deficient cells (the graph summarizes data from a total of four independent experiments; the asterisk indicates $P<0.001$).

morphogenetic events of ECs, we examined the effect of silencing Pfn1 on matrigel-induced cord formation of ECs. HUVECs bearing the control siRNA started spreading as early as 1 hour after seeding on matrigel (data not shown) and formed prominent cord-like structures by 8 hours (Fig. 8A). However, cord formation was significantly inhibited when Pfn1 expression was silenced as evident from the round morphology of majority of Pfn1-deficient cells at the indicated time-point. Quantitative analyses showed that early cord morphogenesis was inhibited by nearly 92% due to loss of Pfn1 expression (Fig. 8B, data summarized from four independent experiments). Even at later time-points (18-22 hours after cell-seeding), we also found the number of cords formed by Pfn1-deficient cells to be still significantly less than that formed in the control culture (data not shown). These data suggest that Pfn1 is a key player in ECM-induced cord morphogenesis of ECs.

Discussion

In the present work, we tested a hypothesis that Pfn1's function is important for EC proliferation and migration. Specifically, we examined the effects of silencing Pfn1 expression on actin cytoskeleton, cell-cell and cell-matrix adhesion, proliferation, migration and consequently, on ECM-induced early cord morphogenesis in vitro.

Consistent with previous findings reported for smooth muscle (Tang and Tan, 2003) and alveolar epithelial (Bitko et al., 2003) cells, we observed a significant reduction of F-actin level in HUVECs when Pfn1 expression was silenced thus implying that Pfn1 promotes actin polymerization in ECs. By contrast, a previous study had shown that gene deletion of Pfn1 and Pfn2 resulted in increased actin polymerization in *Dictyostelium* amoeba thus meaning Pfn's function as G-actin sequestering proteins in this organism (Haugwitz et al., 1994). Cell-specific difference in Pfn's net action on actin cytoskeleton is not surprising since whether Pfn1 would function as a promoter of actin polymerization or a G-actin sequester depends on its concentration relative to that of available G-actin and free barbed ends of actin filaments. These parameters are controlled by other ABPs (sequestering, severing and capping), expression of which can vary between different cell types. Also, in mammalian cells, the intracellular concentration of Pfn1 does not appear to be sufficient for G-actin sequestration, which is primarily regulated by proteins belonging to the thymosin-β family. From reduced actin stress-fibers in Pfn1-deficient cells, it is not immediately clear whether lack of Pfn1 inhibits only actin polymerization or affects the bundling of actin stress-fibers as well. It is known that Diaphanous-family proteins, such as mDia1, utilize Pfn1 to polymerize actin to form stress-fibers (Romero et al., 2004), which might partly explain reduced actin stress-fibers found in Pfn1-deficient cells. Bundling of actin stress-fibers, on the other hand, is facilitated by cell-contractility that requires actomyosin interactions. Pfn1-depletion may down-regulate EC-contractility by partially suppressing actin polymerization [also shown previously for smooth muscle cells (Tang and Tan, 2003)] and therefore affect the bundling of actin stress-fibers. Consistent with the loss of actin stress-fibers, silencing Pfn1 expression also suppressed FA assembly in HUVECs. This data seems to be in qualitative agreement with previous findings by us and others where Pfn1-overexpression caused increased substrate-adhesion of breast cancer cells (Roy and Jacobson, 2004) and human aortic ECs (Moldovan et al., 1997). FA formation is initiated through integrin clustering, a process that is driven by both ECM-binding and contractility (Schoenwaelder and Burridge, 1999). Further assembly of FAs involves signaling through FAK (Focal adhesion kinase) and Src that recruits other molecular components to this adhesive structure. Integrin clustering can be diminished in Pfn1-deficient cells because of possible down-regulation of cell contractility. Surface recruitment of integrins can also be affected by Pfn1-dependent changes in cytoskeletal organization as postulated earlier (Moldovan et al., 1997). Furthermore, we earlier showed that Pfn1-overexpression up-regulates tyrosine phosphorylation of FAK and paxillin in breast cancer cells thus suggesting dependence of FAK-signaling on Pfn1's function (Roy and Jacobson, 2004). Thus, recruitment of molecular components to FA may also be influenced by altered FAK signaling in Pfn1-deficient ECs.

An interesting finding of the present study is that in addition to affecting cell-matrix adhesion, loss of Pfn1 expression also influences cell-cell adhesion where, in particular, VEGF-induced dynamics of intercellular junctions is suppressed. Previous studies showed that agonist-induced disruption of intercellular junctions requires Rho-based EC contraction

(Alexander and Elrod, 2002; Bates et al., 2002). If depletion of Pfn1 reduces EC contractility as observed previously for smooth muscle cells (Tang and Tan, 2003), ECs will become resistant to VEGF-induced disruption of cell-cell adhesion. It has been shown that activation of receptor tyrosine kinases, such as VEGF receptor, is stimulated by integrin clustering and cell-contraction (Gingras et al., 2000; Sundberg and Rubin, 1996). Thus, reduced contractility of Pfn1-deficient cells may also modulate the spatial distribution of VEGF-receptors and hence, suppress VEGF signaling by decreasing the receptor activation. Interestingly, we observed increased nuclear staining of ZO-1 in control HUVECs. It was suggested that nuclear localization of ZO-1 inversely correlates with the maturation of tight junction (Gottardi et al., 1996). This may also explain why the baseline ZO-1 staining in control HUVECs appears somewhat more fragmented than the same in Pfn1-deficient cells.

We found significant inhibition of EC migration as a result of loss of Pfn1 expression thus supporting our hypothesis that Pfn1 is an important player of EC migration. The only previous study that directly evaluated how lack of Pfn1 affects the overall cell migration was performed in dictyostelium and thus, the present work is the first demonstration of the effect of loss of Pfn1 expression on the overall migration of any mammalian cell. In dictyostelium, deletion of both Pfn1 and Pfn2 genes resulted in impaired cell motility, and knocking out Pfn1 gene alone failed to produce a phenotype because of functional compensation by Pfn2 gene product (Haugwitz et al., 1994). Since no Pfn2 expression was detected in HUVECs, we were able to see progressive inhibition of EC migration with loss of Pfn1 expression. Data from our spreading and time-lapse experiments confirm previous findings regarding Pfn1's involvement in cell-protrusion (Hajkova et al., 2000; Suetsugu et al., 1998; Suetsugu et al., 1999). Interestingly, a listeria-motility study showed that although Pfn1 increases the efficiency of listeria-induced actin polymerization and hence, the velocity of pathogen movement, it is not one of the essential cellular components needed for initiating motility of pathogens (Loisel et al., 1999). Similarly, our experiments showed that Pfn1-deficient cells are still able to protrude and migrate, but clearly not to the same extent as displayed by the control cells. Detailed analyses of protrusion revealed that ECs lacking Pfn1 are significantly less efficient in maintaining directional persistence of protrusion compared with the control cells. Since stabilization of membrane protrusion requires cell adhesion, significantly reduced formation of adhesion complexes might partly explain the lack of sustenance of protrusion in Pfn1-deficient cells. Previously, membrane targeting of VASP was inversely correlated with the persistence of cell protrusion (Bear et al., 2002). Interestingly, we also observed a much stronger localization of VASP at the leading edge in Pfn1-deficient cells. Because of reduced actin stress-fibers and FAs in Pfn1-deficient cells, one possibility is that VASP is less sequestered to those cellular structures; therefore, there might be an increased availability of VASP for targeting to cell membrane. Despite consistency in observation, without further experiments it is presently not clear whether there is an actual causal relationship between increased membrane targeting of VASP and decreased persistence of protrusion in our case. Our time-lapse data showed that EC translocation is also inhibited when Pfn1 expression is suppressed. Since actomyosin-based contraction drives cell translocation during motility, our data further suggests a possible down-regulation of contractility in Pfn1-deficient cells.

Besides affecting cell migration, loss of Pfn1 expression also inhibited EC growth by 42% without compromising cell survival, at least in the short-term, thus supporting our hypothesis that Pfn1 plays an important role in EC proliferation. Previous studies showed that Pfn1 localizes at the cleavage furrow during cytokinesis and its function is important for cleavage furrow regression (Dean et al., 2005; Suetsugu et al., 1999). Since Pfn1-deficient cells did not display multinuclei (>2) phenotype, our data suggests that Pfn1's function is not essential for cytokinesis of mammalian ECs as it is for some other species including yeast and amoeba (Haugwitz et al., 1994; Lu and Pollard, 2001). The fact that we observed only a partial inhibition of EC proliferation after near complete silencing of Pfn1 gene is intriguing since it has been shown that gene deletion of Pfn1 arrests developing mouse embryo at the two-cell stage and produces embryonic lethality (Witke et al., 2001). Although it is tempting to speculate that embryonic stem cells might be more sensitive to loss of Pfn1 expression, a more detailed work is necessary to address whether persistent suppression of Pfn1 expression completely arrests cell-growth and/or affects the long-term survival of ECs. Future work is also needed to determine the effect of loss of Pfn1 expression on different phases of cell cycle.

Finally, we demonstrated that silencing Pfn1 expression significantly inhibits ECM-induced early cord morphogenesis of ECs. Network formation by ECs on ECM proceeds through several stages including (1) cell adhesion on ECM, (2) cell migration, (3) cell-induced mechanical remodeling of ECM that further defines matrix guidance tracks to allow directed EC migration to the neighboring cells, and (4) cell proliferation (Cascone et al., 2003; Davis et al., 2002; Davis and Camarillo, 1995; Liu and Senger, 2004; Whelan and Senger, 2003). Early impairment in cord-forming ability of Pfn1-deficient ECs is most likely a result of defect in cell migration and not due to delayed cell proliferation. We observed less cord formation by Pfn1-deficient cells also at later time-points (18-22 hours after cell seeding – data not shown) in which case, however, additional contribution of inhibited cell proliferation cannot be ruled out. Directed EC migration on ECM is not only influenced by the intrinsic migratory ability of cells, but also governed by the ECM-remodeling capacity of cells. Reduced formation of actin stress-fibers and FAs might render Pfn1-deficient cells less efficient in ECM remodeling because of possible down-regulation of contractility. One also needs to consider a possible influence of Pfn1-dependent modulation of cell-cell adhesion on cord formation. Although cadherin-mediated junctions are important for endothelial assembly and capillary formation, early events of capillary morphogenesis of EC involve disruptions of cell-cell contacts that are presumably critical for both EC migration and alignment to form pre-capillary cords (Carmeliet, 2000; Liu and Senger, 2004). Our data showed that both control and Pfn1-deficient cells are capable of forming cell-cell adhesions; however, the latter display reduced dynamics of cell-cell adhesions when challenged with VEGF. Thus, altered dynamics of cell-cell adhesion due to loss of Pfn1 expression can have an inhibitory effect on EC migration. Finally, our wound-healing data showed that cell migration is only partially inhibited by silencing Pfn1 expression. Thus, it is not surprising that cells lacking Pfn1 are still able to form cords

but to a much lesser extent compared with the control cells. In conclusion, since cord morphogenesis is an early endothelial rearrangement necessary for capillary formation by ECs, results of the present work justify further studies to explore whether Pfn1 plays a role in capillary morphogenesis of ECs.

Materials and Methods

Antibodies and reagents

Polyclonal antibodies specific for Pfn1 and Pfn2 were generous gifts of Drs Sally Zigmond (University of Pennsylvania) and Walter Witke (European Molecular Biology Laboratory, Italy), respectively. Polyclonal antibody for N-WASP was kindly provided by Dr Hideki Yamaguchi (Albert Einstein College of Medicine). Monoclonal antibodies for VASP and ZO-1 (zonula occludens-1) were obtained from Pharmingen (San Diego, CA). Monoclonal antibodies for GAPDH and actin are products of Chemicon (Temecula, CA). Monoclonal antibody for vinculin is a product of Sigma (St Louis, MO). Polyclonal antibody for mDia1 was obtained from Abcam (Cambridge, MA). Monoclonal antibody for VE-cadherin (vascular endothelial cadherin) was obtained from Santa Cruz Biotechnology (Santa Cruz, CA). For immunoblotting, the antibodies were used at the following concentrations: Pfn1 (1:500), Pfn2 (1:1000), VASP (1:500), GAPDH (1:200), actin (1:1000), ZO-1 (1:500), VE-cadherin (1:1000), N-WASP (1:1000), and mDia1 (1:2500). Rhodamine-phalloidin and DAPI were purchased from Molecular Probes (Carlsbad, CA). Collagen type I and growth-factor-reduced matrigel are products of BD Biosciences (Bedford, MA).

Cell culture and transfection

HUVECs (source: Cambrex Biosciences, Walkersville, MD) were cultured in the complete EBM2 growth media (also commercially available from the same source). To silence Pfn1 expression, a custom-designed siRNA (sense strand: 5′-AGA AGG UGU CCA CGG UGG UUU-3′; antisense-strand: 5′-ACC ACC GUG GAC ACC UUC UUU-3′) was synthesized by Dharmacon (Lafayette, CO) and was transfected into HUVECs using a proprietary reagent according to the manufacturer's protocol. A control siRNA (sense strand 5′-UAG CGA CUA AAC ACA UCA AUU-3′; antisense strand: 5′-UUG AUG UGU UUA GUC GCU AUU-3′) that bears no significant homology with any known mouse or human gene and commercially available from the same source was used for the control experiments. Briefly, ECs were transfected with 100 nM of siRNA for 24 hours. The transfection media was then replaced with the regular growth media and cells were cultured for another 24-72 hours before performing the experiments.

Protein extraction and immunoblotting

For protein extraction, cells were washed twice with cold PBS and lysed on ice for 30 minutes in modified RIPA buffer containing 50 mM Tris-HCl (pH 7.5), 150 mM NaCl, 1% NP-40, 0.5% sodium deoxycholate, 0.1% SDS, 2 mM EDTA, 50 mM NaF, 1 mM sodium pervanadate, and protease inhibitors (10 μg/ml of leupeptin, aprotinin, pepstatin and 1 mM phenylmethylsulfonyl fluoride). The lysates were clarified at ~17,000 ***g*** for 15 minutes at 4°C and the protein concentration was determined using a Coomassie-based protein assay kit (Pierce; Rockford, IL). Proteins separated on SDS-PAGE were transferred onto a nitrocellulose membrane. After blocking the membrane with 5% non-fat dry milk in TBST for 1 hour at room temperature, immunoblotting was performed by overnight incubation with the appropriate primary antibodies. After extensive washing with TBST, the blot was incubated with the appropriate secondary antibody (Pharmingen, San Diego, CA) and washed three times with TBST before performing chemiluminescence for visualization of protein bands.

Immunostaining

For VASP and vinculin immunostaining, cells cultured on collagen-coated coverslips were washed 3 times with PBS, fixed with 3.7% formaldehyde for 15 minutes, permeablized with 0.5% Triton X-100 for 5 minutes and then blocked with 10% goat-serum for 30 minutes. After incubating with the primary antibody at a 1:100 dilution for 1 hour at room temperature, cells were washed four times (first twice with PBS containing 0.02% tween and then twice with PBS), each of 3-minute duration, before incubating with a FITC-conjugated anti-mouse secondary antibody (1:100 dilution). For VE-cadherin and ZO-1 staining, cells were fixed and permeabilized using cold methanol at –20°C for 20 minutes and then blocked with 5% BSA (containing 15% glycine) for 45 minutes at room temperature. After incubating with either VE-cadherin (1:200 dilution) or ZO-1 (1:250 dilution) antibody for 1 hour at room temperature, cells were washed five times with 5% BSA (containing 15% glycine) followed by washing five times with PBS before incubating with the appropriate secondary antibody. Stained cells were then washed five times using similar procedures. Fluorescence microscopy of immunostained cells was performed on an IX-71 Olympus inverted microscope where all images were acquired using the Metamorph imaging software.

F-actin quantification

To visualize F-actin, cells were stained with rhodamine-phalloidin using standard protocol and imaged using a 60× objective. For quantification of fluorescence, we acquired images of phalloidin-stained cells at 6-12 random fields of observation in each experiment using a 20× objective. After performing background subtraction of the images, we calculated the average fluorescence intensity per cell for each field of observation. These values were then normalized with respect to the average fluorescence value calculated for the control cells for a given experiment. Normalized fluorescence data of control and Pfn1-siRNA treated cells were pooled from two experiments, the average values of which were then statistically compared using a Student's *t*-test.

Cell-proliferation assay

HUVECs were plated in triplicate at a density of 20,000 cells per well of a 24-well plate 24 hours after transfection with the appropriate siRNAs. At different time-points after transfection (48-96 hours), cells were washed with PBS and stained with 0.5% crystal violet for 15 minutes. After washing cells three times with PBS, dye was eluted from cells by adding 300 μl of 100% ethanol in each well and its absorbance was measured using a plate-reader. Absorbance data based on triplicate set of samples for each experimental condition from a total of three independent experiments were then averaged for statistical comparison using a Student's *t*-test.

Cell spreading assay

HUVECs were plated on the wells of a 24-well plate that were pre-coated with different concentrations of matrigel (25 and 100 μg/ml) and the percentages of cells that showed spreading morphology (appears phase-dense) were determined at different time-points (30 and 60 minutes) after cell seeding. Percentage of spreading cells was calculated in each of the three random fields of observation and averaged based on data from two independent experiments for statistical comparison using a Student's *t*-test.

Wound healing assay

Confluent monolayers of HUVECs cultured in the wells of a 24-well plate was mechanically scratched using a pipette tip. Cell debris was removed by washing with PBS before adding complete growth media to the cells. Images of the wound edges were acquired at three random locations first immediately after wounding and then at the same locations after 12 hours to assess the wound closure by migrating HUVECs. Wound closure was quantified by the percentage change in the wound area per unit time and averaged for three locations per well from a triplicate set of samples for each experimental condition. This assay was performed 48, 72 and 96 hours after siRNA transfection.

Single-cell migration assay

HUVECs transfected with the appropriate siRNAs were sparsely plated on a 35 mm tissue-culture dish and after an overnight incubation, time-lapse videomicroscopy of three random fields were simultaneously performed at an interval of 3 minutes for a total duration of 90 minutes. The acquired images were analyzed using ImageJ and Metamorph softwares.

Cord formation assay

Two-hundred microliters of matrigel was polymerized in the wells of a 48-well plate at 37°C for 30 minutes prior to seeding 25,000 HUVECs on top of matrigel, and early cord morphogenesis of ECs was assessed after 8 hours by phase-contrast microscopy. Cord-formation data was quantified by counting the number of nodes in a given field of observation that had at least three branches (Shen et al., 2005), which was then averaged for three fields per well from a duplicate set of samples for each experimental condition. These data were statistically compared using a Student's *t*-test.

We thank Anna DiRienzo for critically reading the manuscript. This work is supported by grants from the National Institute of Health (CA108607-01), American Heart Association, Central Research Development and Competitive Medical Research funds of the University of Pittsburgh (to P.R.).

References

Alexander, J. S. and Elrod, J. W. (2002). Extracellular matrix, junctional integrity and matrix metalloproteinase interactions in endothelial permeability regulation. *J. Anat.* **200**, 561-574.

Bates, D. O., Hillman, N. J., Williams, B., Neal, C. R. and Pocock, T. M. (2002). Regulation of microvascular permeability by vascular endothelial growth factors. *J. Anat.* **200**, 581-597.

Bear, J. E., Svitkina, T. M., Krause, M., Schafer, D. A., Loureiro, J. J., Strasser, G. A., Maly, I. V., Chaga, O. Y., Cooper, J. A., Borisy, G. G. et al. (2002). Antagonism between Ena/VASP proteins and actin filament capping regulates fibroblast motility. *Cell* **109**, 509-521.

Bitko, V., Oldenburg, A., Garmon, N. E. and Barik, S. (2003). Profilin is required for viral morphogenesis, syncytium formation, and cell-specific stress fiber induction by respiratory syncytial virus. *BMC Microbiol.* **3**, 9.

Boettner, B., Govek, E. E., Cross, J. and Van Aelst, L. (2000). The junctional multidomain protein AF-6 is a binding partner of the Rap1A GTPase and associates with the actin cytoskeletal regulator profilin. *Proc. Natl. Acad. Sci. USA* **97**, 9064-9069.

Buss, F., Temm-Grove, C., Henning, S. and Jockusch, B. M. (1992). Distribution of profilin in fibroblasts correlates with the presence of highly dynamic actin filaments. *Cell Motil. Cytoskeleton* **22**, 51-61.

Carlsson, L., Nystrom, L. E., Sundkvist, I., Markey, F. and Lindberg, U. (1977). Actin polymerizability is influenced by profilin, a low molecular weight protein in non-muscle cells. *J. Mol. Biol.* **115**, 465-483.

Carmeliet, P. (2000). Mechanisms of angiogenesis and arteriogenesis. *Nat. Med.* **6**, 389-395.

Carmeliet, P. and Jain, R. K. (2000). Angiogenesis in cancer and other diseases. *Nature* **407**, 249-257.

Cascone, I., Giraudo, E., Caccavari, F., Napione, L., Bertotti, E., Collard, J. G., Serini, G. and Bussolino, F. (2003). Temporal and spatial modulation of Rho GTPases during in vitro formation of capillary vascular network. Adherens junctions and myosin light chain as targets of Rac1 and RhoA. *J. Biol. Chem.* **278**, 50702-50713.

Cha, H. J., Jeong, M. J. and Kleinman, H. K. (2003). Role of thymosin beta4 in tumor metastasis and angiogenesis. *J. Natl. Cancer Inst.* **95**, 1674-1680.

Chou, J., Stolz, D. B., Burke, N. A., Watkins, S. C. and Wells, A. (2002). Distribution of gelsolin and phosphoinositol 4,5-bisphosphate in lamellipodia during EGF-induced motility. *Int. J. Biochem. Cell Biol.* **34**, 776-790.

Davis, G. E. and Camarillo, C. W. (1995). Regulation of endothelial cell morphogenesis by integrins, mechanical forces, and matrix guidance pathways. *Exp. Cell Res.* **216**, 113-123.

Davis, G. E., Black, S. M. and Bayless, K. J. (2000). Capillary morphogenesis during human endothelial cell invasion of three-dimensional collagen matrices. *In Vitro Cell. Dev. Biol. Anim.* **36**, 513-519.

Davis, G. E., Bayless, K. J. and Mavila, A. (2002). Molecular basis of endothelial cell morphogenesis in three-dimensional extracellular matrices. *Anat. Rec.* **268**, 252-275.

Dean, S. O., Rogers, S. L., Stuurman, N., Vale, R. D. and Spudich, J. A. (2005). Distinct pathways control recruitment and maintenance of myosin II at the cleavage furrow during cytokinesis. *Proc. Natl. Acad. Sci. USA* **102**, 13473-13478.

Di Nardo, A., Gareus, R., Kwiatkowski, D. and Witke, W. (2000). Alternative splicing of the mouse profilin II gene generates functionally different profilin isoforms. *J. Cell Sci.* **113**, 3795-3803.

Gingras, D., Lamy, S. and Beliveau, R. (2000). Tyrosine phosphorylation of the vascular endothelial-growth-factor receptor-2 (VEGFR-2) is modulated by Rho proteins. *Biochem. J.* **348**, 273-280.

Gottardi, C. J., Arpin, M., Fanning, A. S. and Louvard, D. (1996). The junction-associated protein, zonula occludens-1, localizes to the nucleus before the maturation and during the remodeling of cell-cell contacts. *Proc. Natl. Acad. Sci. USA* **93**, 10779-10784.

Grant, D. S., Kinsella, J. L., Kibbey, M. C., LaFlamme, S., Burbelo, P. D., Goldstein, A. L. and Kleinman, H. K. (1995). Matrigel induces thymosin beta 4 gene in differentiating endothelial cells. *J. Cell Sci.* **108**, 3685-3694.

Grant, D. S., Rose, W., Yaen, C., Goldstein, A., Martinez, J. and Kleinman, H. (1999). Thymosin beta4 enhances endothelial cell differentiation and angiogenesis. *Angiogenesis* **3**, 125-135.

Grenklo, S., Geese, M., Lindberg, U., Wehland, J., Karlsson, R. and Sechi, A. S. (2003). A crucial role for profilin-actin in the intracellular motility of Listeria monocytogenes. *EMBO Rep.* **4**, 523-529.

Gronborg, M., Kristiansen, T. Z., Iwahori, A., Chang, R., Reddy, R., Sato, N., Molina, H., Jensen, O. N., Hruban, R. H., Goggins, M. G. et al. (2006). Biomarker discovery from pancreatic cancer secretome using a differential proteomic approach. *Mol. Cell Proteomics* **5**, 157-171.

Hajkova, L., Nyman, T., Lindberg, U. and Karlsson, R. (2000). Effects of cross-linked profilin:beta/gamma-actin on the dynamics of the microfilament system in cultured cells. *Exp. Cell Res.* **256**, 112-121.

Haugwitz, M., Noegel, A. A., Karakesisoglou, J. and Schleicher, M. (1994). Dictyostelium amoebae that lack G-actin-sequestering profilins show defects in F-actin content, cytokinesis, and development. *Cell* **79**, 303-314.

Hu, E., Chen, Z., Fredrickson, T. and Zhu, Y. (2001). Molecular cloning and characterization of profilin-3: a novel cytoskeleton-associated gene expressed in rat kidney and testes. *Exp. Nephrol.* **9**, 265-274.

Janke, J., Schluter, K., Jandrig, B., Theile, M., Kolble, K., Arnold, W., Grinstein, E., Schwartz, A., Estevez-Schwarz, L., Schlag, P. M. et al. (2000). Suppression of tumorigenicity in breast cancer cells by the microfilament protein profilin 1. *J. Exp. Med.* **191**, 1675-1686.

Kanda, S., Miyata, Y. and Kanetake, H. (2004). Role of focal adhesion formation in migration and morphogenesis of endothelial cells. *Cell. Signal.* **16**, 1273-1281.

Kwiatkowski, D. J. and Bruns, G. A. (1988). Human profilin. Molecular cloning, sequence comparison, and chromosomal analysis. *J. Biol. Chem.* **263**, 5910-5915.

Lambrechts, A., Braun, A., Jonckheere, V., Aszodi, A., Lanier, L. M., Robbens, J., Van Colen, I., Vandekerckhove, J., Fassler, R. and Ampe, C. (2000). Profilin II is alternatively spliced, resulting in profilin isoforms that are differentially expressed and have distinct biochemical properties. *Mol. Cell. Biol.* **20**, 8209-8219.

Laurent, V., Loisel, T. P., Harbeck, B., Wehman, A., Grobe, L., Jockusch, B. M., Wehland, J., Gertler, F. B. and Carlier, M. F. (1999). Role of proteins of the Ena/VASP family in actin-based motility of Listeria monocytogenes. *J. Cell Biol.* **144**, 1245-1258.

Lederer, M., Jockusch, B. M. and Rothkegel, M. (2005). Profilin regulates the activity of p42POP, a novel Myb-related transcription factor. *J. Cell Sci.* **118**, 331-341.

Liu, Y. and Senger, D. R. (2004). Matrix-specific activation of Src and Rho initiates capillary morphogenesis of endothelial cells. *FASEB J.* **18**, 457-468.

Loisel, T. P., Boujemaa, R., Pantaloni, D. and Carlier, M. F. (1999). Reconstitution of actin-based motility of Listeria and Shigella using pure proteins. *Nature* **401**, 613-616.

Lu, J. and Pollard, T. D. (2001). Profilin binding to poly-L-proline and actin monomers along with ability to catalyze actin nucleotide exchange is required for viability of fission yeast. *Mol. Biol. Cell* **12**, 1161-1175.

Malinda, K. M., Goldstein, A. L. and Kleinman, H. K. (1997). Thymosin beta 4 stimulates directional migration of human umbilical vein endothelial cells. *FASEB J.* **11**, 474-481.

Mimuro, H., Suzuki, T., Suetsugu, S., Miki, H., Takenawa, T. and Sasakawa, C. (2000). Profilin is required for sustaining efficient intra- and intercellular spreading of Shigella flexneri. *J. Biol. Chem.* **275**, 28893-28901.

Moldovan, N. I., Milliken, E. E., Irani, K., Chen, J., Sohn, R. H., Finkel, T. and Goldschmidt-Clermont, P. J. (1997). Regulation of endothelial cell adhesion by profilin. *Curr. Biol.* **7**, 24-30.

Neely, M. D. and Macaluso, E. (1997). Motile areas of leech neurites are rich in microfilaments and two actin-binding proteins: gelsolin and profilin. *Proc. Biol. Sci.* **264**, 1701-1706.

Neuhoff, H., Sassoe-Pognetto, M., Panzanelli, P., Maas, C., Witke, W. and Kneussel, M. (2005). The actin-binding protein profilin I is localized at synaptic sites in an activity-regulated manner. *Eur. J. Neurosci.* **21**, 15-25.

Obermann, H., Raabe, I., Balvers, M., Brunswig, B., Schulze, W. and Kirchhoff, C. (2005). Novel testis-expressed profilin IV associated with acrosome biogenesis and spermatid elongation. *Mol. Hum. Reprod.* **11**, 53-64.

Philp, D., Goldstein, A. L. and Kleinman, H. K. (2004). Thymosin beta4 promotes angiogenesis, wound healing, and hair follicle development. *Mech. Ageing Dev.* **125**, 113-115.

Pollard, T. D. and Borisy, G. G. (2003). Cellular motility driven by assembly and disassembly of actin filaments. *Cell* **112**, 453-465.

Reinhard, M., Giehl, K., Abel, K., Haffner, C., Jarchau, T., Hoppe, V., Jockusch, B. M. and Walter, U. (1995). The proline-rich focal adhesion and microfilament protein VASP is a ligand for profilins. *EMBO J.* **14**, 1583-1589.

Romero, S., Le Clainche, C., Didry, D., Egile, C., Pantaloni, D. and Carlier, M. F. (2004). Formin is a processive motor that requires profilin to accelerate actin assembly and associated ATP hydrolysis. *Cell* **119**, 419-429.

Roy, P. and Jacobson, K. (2004). Overexpression of profilin reduces the migration of invasive breast cancer cells. *Cell Motil. Cytoskeleton* **57**, 84-95.

Salazar, R., Bell, S. E. and Davis, G. E. (1999). Coordinate induction of the actin cytoskeletal regulatory proteins gelsolin, vasodilator-stimulated phosphoprotein, and profilin during capillary morphogenesis in vitro. *Exp. Cell Res.* **249**, 22-32.

Sanger, J. M., Mittal, B., Southwick, F. S. and Sanger, J. W. (1995). Listeria monocytogenes intracellular migration: inhibition by profilin, vitamin D-binding protein and DNase I. *Cell Motil. Cytoskeleton* **30**, 38-49.

Schluter, K., Jockusch, B. M. and Rothkegel, M. (1997). Profilins as regulators of actin dynamics. *Biochim. Biophys. Acta* **1359**, 97-109.

Schoenwaelder, S. M. and Burridge, K. (1999). Bidirectional signaling between the cytoskeleton and integrins. *Curr. Opin. Cell Biol.* **11**, 274-286.

Shen, T. L., Park, A. Y., Alcaraz, A., Peng, X., Jang, I., Koni, P., Flavell, R. A., Gu, H. and Guan, J. L. (2005). Conditional knockout of focal adhesion kinase in endothelial cells reveals its role in angiogenesis and vascular development in late embryogenesis. *J. Cell Biol.* **169**, 941-952.

Suetsugu, S., Miki, H. and Takenawa, T. (1998). The essential role of profilin in the assembly of actin for microspike formation. *EMBO J.* **17**, 6516-6526.

Suetsugu, S., Miki, H. and Takenawa, T. (1999). Distinct roles of profilin in cell morphological changes: microspikes, membrane ruffles, stress fibers, and cytokinesis. *FEBS Lett.* **457**, 470-474.

Sundberg, C. and Rubin, K. (1996). Stimulation of beta1 integrins on fibroblasts induces PDGF independent tyrosine phosphorylation of PDGF beta-receptors. *J. Cell Biol.* **132**, 741-752.

Tang, D. D. and Tan, J. (2003). Downregulation of profilin with antisense oligodeoxynucleotides inhibits force development during stimulation of smooth muscle. *Am. J. Physiol. Heart Circ. Physiol.* **285**, H1528-H1536.

Theriot, J. A., Rosenblatt, J., Portnoy, D. A., Goldschmidt-Clermont, P. J. and Mitchison, T. J. (1994). Involvement of profilin in the actin-based motility of L. monocytogenes in cells and in cell-free extracts. *Cell* **76**, 505-517.

Verheyen, E. M. and Cooley, L. (1994). Profilin mutations disrupt multiple actin-dependent processes during Drosophila development. *Development* **120**, 717-728.

Watanabe, N., Madaule, P., Reid, T., Ishizaki, T., Watanabe, G., Kakizuka, A., Saito, Y., Nakao, K., Jockusch, B. M. and Narumiya, S. (1997). p140mDia, a mammalian homolog of Drosophila diaphanous, is a target protein for Rho small GTPase and is a ligand for profilin. *EMBO J.* **16**, 3044-3056.

Whelan, M. C. and Senger, D. R. (2003). Collagen I initiates endothelial cell morphogenesis by inducing actin polymerization through suppression of cyclic AMP and protein kinase A. *J. Biol. Chem.* **278**, 327-334.

Witke, W. (2004). The role of profilin complexes in cell motility and other cellular processes. *Trends Cell Biol.* **14**, 461-469.

Witke, W., Sutherland, J. D., Sharpe, A., Arai, M. and Kwiatkowski, D. J. (2001). Profilin I is essential for cell survival and cell division in early mouse development. *Proc. Natl. Acad. Sci. USA* **98**, 3832-3836.

Yancopoulos, G. D., Davis, S., Gale, N. W., Rudge, J. S., Wiegand, S. J. and Holash, J. (2000). Vascular-specific growth factors and blood vessel formation. *Nature* **407**, 242-248.